



## OPEN ZFP1 is a biomarker related to poor prognosis and immunity in gastric cancer

Jibin Yao<sup>1,2,5</sup>, Fubin Ma<sup>3,5</sup>, Donghai Shi<sup>4</sup> & Mingxu Da<sup>1,2</sup>✉

We aimed to determine the prognostic significance of ZFP1 in gastric cancer (GC), its role in the immune microenvironment, and its potential as a therapeutic target using data from The Cancer Genome Atlas (TCGA) database. ZFP1 overexpression was closely associated with tumour T stage and histological grade. Patients with GC and high ZFP1 expression had poor outcomes. Lower ZFP1 expression was associated with longer symptom-free intervals and disease-specific survival. Subgroup analyses of T3 and T4, N0, N1, and M0 patients showed that overall survival (OS), disease-specific survival, and progression-free interval (PFI) were worse in those with high ZFP1 expression. ZFP1 expression in GC was moderately to strongly positively correlated with the infiltration levels of effector central memory T cells and T helper cells and negatively correlated with Th17 cells and NK CD56bright cells. The lncRNA-miRNA-ZFP1 axis was predicted using a public database. CCK8, colony formation, and wound healing assays were conducted to investigate whether ZFP1 promoted the proliferation and migration of GC cells. Our study suggests that ZFP1 plays a key role in the prognosis, immune response, and progression of GC and is a significant factor in the diagnosis and treatment of this disease.

**Keywords** Biomarker, ZFP1, Gastric cancer, Prognosis, Immune infiltration

Globally, gastric cancer (GC) is the fifth most common malignant tumour in terms of incidence and the fourth leading cause of cancer-related mortality. Although the incidence and mortality rates have declined, in 2020, there were 769,000 deaths worldwide from GC and more than 1 million new cases<sup>1</sup>. In ageing populations, clinicians encounter more patients with cancer compared to younger populations. Early diagnosis can substantially improve the survival rate of patients with GC; however, owing to the limitations of techniques such as liquid biopsy, the most important clinical modality for early diagnosis remains invasive gastroscopic biopsy<sup>2</sup>. GC tissues are highly heterogeneous and complex, and there is a lack of effective biomarkers to diagnose and predict the prognosis of GC. Therefore, the discovery of new molecules with diagnostic and therapeutic value is a priority in GC research<sup>3</sup>.

Kruppel-associated box structural domain zinc finger proteins (KZFPs) represent the largest transcriptional regulatory family of genes encoded by higher vertebrates<sup>4</sup>. The human genome can encode hundreds of KZFPs. These proteins are characterized by N-terminal KRAB structural domains and C-terminal DNA-binding zinc finger arrays. Together with their cofactors, KZFPs are involved in the repression of transposable element-derived sequences during epigenetic reprogramming in the first few days of embryogenesis<sup>5</sup>. Initially, the evolutionary selection of KZFPs was thought to be a host component of the arms race against transposable elements. However, research has found that KZFPs play crucial regulatory roles in biological processes such as development, physiology, and tumours in chordates<sup>4,5</sup>. The zinc finger protein (ZFP) plays an important role in gastric carcinogenesis and progression<sup>6</sup>.

ZFP1 (ZFP1 ZFP), also known as ZNF475, belongs to the family of ZFPs first discovered in mice<sup>7</sup>, and later identified in human tissues. ZFP1 enters the nucleus and plays an important role in transcriptional regulation during early embryonic development<sup>8</sup>. ZFP1 and its homologue MLLT10 (also known as AF10) contain a PHD1-PHD2 structural domain that is highly conserved among proteins<sup>9</sup>. MLLT10 has been found to play a significant pro-carcinogenic role in leukaemia<sup>10</sup> and colon cancer<sup>11</sup>. Patients with laryngeal cancer and high ZFP1 expression

<sup>1</sup>The First School of Clinical Medicine, Lanzhou University, No.204 Donggang West Road, Lanzhou 730000, People's Republic of China. <sup>2</sup>Department of Surgical Oncology, Gansu Province Hospital, Lanzhou, People's Republic of China. <sup>3</sup>Department of Surgery, Ningxia Medical University, Yinchuan, People's Republic of China. <sup>4</sup>The First School of Clinical Medicine, Gansu University of Chinese Medicine, Lanzhou, People's Republic of China. <sup>5</sup>These authors contributed equally: Jibin Yao and Fubin Ma. ✉email: ldy\_damx@lzu.edu.cn

had a worse prognosis<sup>12</sup>. However, studies on the effects of ZFP1 in cancer are limited, and the role of ZFP1 in the mechanism and progression of GC has not been reported.

In this study, we investigated the relationship between ZFP1 expression and clinicopathological features of GC, determined the prognostic value of ZFP1 in patients with GC, and explored the possible mechanisms by which ZFP1 expression affects GC development.

## Materials and methods

### Data collection and clinical samples

Stomach adenocarcinoma (STAD) data were downloaded from the TCGA database, and insufficient or missing data were deleted. Three hundred seventy-five patients with GC and 32 normal samples were included for ZFP1 expression and survival data analysis. The GEO datasets GSE15459, GSE22377, GSE51105, and GSE62254 were used for external validation. Twenty patients with GC who underwent radical gastrectomy at Gansu Provincial Hospital were included. All patients were diagnosed with GC, confirmed by preoperative pathological examination, and did not receive preoperative antitumour therapy. This research project was approved by the Ethics Committee of Gansu Provincial People Hospital (2023-312, 20230727) and authorised by all patients. The HPA database (<https://www.proteinatlas.org/>) was used to verify ZFP1 protein expression.

### Expression of ZFP1 in GC from the TCGA database

Statistical analysis was performed using R language (version 4.2.1). Data were visualised using the ggplot2 package to clarify the differential expression of ZFP1. The differential gene (DEG) threshold was  $|\log_{2}FC| > 2.0$  and adjusted to  $p < 0.05$ . A receiver operating characteristic (ROC) curve was used to assess the diagnostic value of ZFP1.

### Analysis clinicopathologic features and survival

The Wilcoxon signed rank sum test, logistic regression, and multivariate Cox analysis were used to analyse the correlation between clinicopathological characteristics and ZFP1. The effect of ZFP1 on survival was assessed using Cox regression and Kaplan–Meier analyses. The nomogram predicted survival at 1 year and 3 years.

### Enrichment analysis and protein interaction (PPI) network

Biological processes, cellular components, and Kyoto Encyclopedia of Genes and Genomes (KEGG) analysis were performed using the clusterProfiler package (version 4.4.4) GO plot (1.0.2) in R<sup>13,14</sup>. The cluster analysis software package (version 4.4.4) was used for GSEA analysis<sup>15</sup>. Adjusted  $p < 0.05$  and FDR  $< 0.25$  were considered statistically significant. The STING database (<https://string-db.org/>) was used to construct a PPI network of DEGs to assess protein interactions of ZFP1.

### Immune infiltration analysis

Immune infiltration based on differences in ZFP1 mRNA expression was analyzed using an independent sample *t*-test. Immunization scores were calculated using the R software package (version 1.0.13) and the analysis was visualized in lollipop plots by using the ggplot2 package<sup>16</sup>. Correlations between ZFP1 and 24 immune cell types were elucidated using Spearman's correlation<sup>17</sup>.

### Prediction and analysis of lncRNA-miRNA-ZFP1 regulatory network

MiRDB ([www.mirdb.org](http://www.mirdb.org)), TargetScan Human 7.0 ([www.targetscan.org](http://www.targetscan.org)), and miRWalk (<http://mirwalk.umm.uniheidelberg.de/>), miRTarbase (<http://mirtarbase.mbc.nctu.edu.tw/index.html>) were used to predict the upstream binding miRNAs of ZFP1. ENCORI (<https://rnasyu.com/encori/index.php>) was used to predict lncRNAs that bind to miR-27a-3p and perform an intergenic correlation analysis. Cytoscape 3.9.0 software was used to analyse and plot the lncRNA-miRNA-ZFP1 regulatory network.

### Cell culture

The HGC27 and MKN45 cell lines were purchased from the Shanghai Cell Bank. RPMI 1640 medium (BI, IL, USA) was supplemented with 10% FBS (Wilber, China). The parameters of the incubator were set to 5% CO<sub>2</sub> concentration, 37 °C constant temperature, and 95% humidity.

### RNA interference

The siRNA-ZFP1 was synthesised by HANBI (Shanghai, China). The sequences were as follows: si-ZFP1-1, sense: 5'-GGAGAAUUAUAGCAACUUATT-3'; si-ZFP1-2, sense: 5'-CAGACUUGC UUAAUAGUAATT-3'; and si-ZFP1-3, sense: 5'-GAGUGUAACGAAUGUGCAATT-3'. Transfection was performed by adding siRNA transfection complexes to RNAFit (HANBI).

### IHC

ZFP1 expression in GC specimens was detected using IHC. Sections were incubated using ZFP1 polyclonal antibody (1:1000) (Thermo Fisher, USA) overnight at 4 °C and the secondary antibody (Jackson, USA) for 1 h at room temperature. Protein expression was determined as follows: staining intensity score (0, unstained; 1, light; 2, brown; 3, tan) and positive cell number score (0 points for 0%-5%; 1 point for 6%-25%; 2 points for 26%-50%; 3 points for > 50%). The sum of these two fractions was used to semi-quantify ZFP1 expression: > 3 was classified as positive, and ≤ 3 was classified as negative. Two experienced pathologists performed independent scoring in a double-blind manner.

### Western blotting

Protein concentration was determined using the BSA method after protein extraction with radioimmunoprecipitation assay (RIPA) buffer (Bosterbio, China). Proteins were separated using 10% sodium dodecyl sulfate–polyacrylamide gel electrophoresis and transferred to PVDF membranes. After electrophoresis and membrane transfer, ZFP1 primary antibody (Thermo Fisher, USA) was added overnight at 4 °C, followed by incubation with a secondary antibody (Jackson, USA).

### CCK8

The 96-well plates were filled with  $5 \times 10^3$  treated cells, followed by CCK8 (Apexbio, USA). A microplate reader (Thermo Fisher, USA) was used for measurements at 450 nm. For the clone formation assay, 600 treated cells were added to a 6-well plate. Two weeks later, formaldehyde fixation for 30 min and 0.1% staining for 20 min were performed to observe colony formation.

### EdU

HGC-27 and MKN45 cells were seeded into 6-well plates, and cell proliferation was detected after 2 h by using the EdU assay (Bergolin, China), according to the manufacturer's instructions. Finally, fluorescence images of the GC cells were captured using an Olympus fluorescence microscope.

### Wound healing assays

A wound healing assay was used to evaluate cell migration capacity. Scratches were made with the same 200  $\mu$ L micropipette tip, rinsed with PBS, and added to a serum-free medium. Images were captured at 0, 24, and 48 h.

### Transwell

GC cells ( $5 \times 10^4$  GC cells were added to the upper chamber with Matrigel (Mei5Bio, China) for the migration assay or without Matrigel for the invasion assay. RPMI 1640 medium (BI, IL, USA) containing 20% FBS was used to fill the lower chambers. After 48 h (migration) or 72 h (invasion), non-migrating or non-invading cells were carefully removed. The migrated cells were fixed with 4% paraformaldehyde, stained with 0.1% crystal violet, and observed under a fluorescence microscope.

### miRNA pull-down

A biotin-labelled miR-27a-3p fragment was synthesised, and MKN45 cells were transfected and cultured for 36 h. The cells were lysed, captured, and enriched using streptavidin-coupled magnetic beads, and the target miRNA was obtained after elution and purification. qPCR was performed to detect the expression levels of KCNQ1OT1 and ZFP1. The expression of KCNQ1OT1 and ZFP1 was detected using qPCR.

## Result

### Clinical baseline information

In the TCGA database, the characteristics of GC patients were analysed, such as age, sex, TNM stage, and primary therapy outcome (Table 1). The 375 patients were divided into the ZFP1 high- and low-expression groups (188 and 187, respectively). Poor prognostic features, including T stage and histological grade, were associated with ZFP1 expression.

### High expression of ZFP1 in STAD

Combining the databases of TCGA and GTEx enabled pan-cancer analysis of ZFP1. ZFP1 was significantly expressed in adrenocortical carcinoma (ACC), breast invasive carcinoma (BRCA), lymphoid neoplasm diffuses large B-cell lymphoma (DLBC), oesophageal carcinoma (ESCA), glioblastoma multiforme (GBM), head and neck squamous cell carcinoma (HNSC), kidney renal papillary cell carcinoma (KIRP), lung adenocarcinoma (LUAD), lung squamous cell carcinoma (LUSC), pancreatic adenocarcinoma (PAAD), STAD, skin cutaneous melanoma (SKCM), thyroid carcinoma (THCA), and thymoma (THYM) ( $p < 0.05$ ) (Fig. 1A).

Next, we analysed ZFP1 expression in 375 GC tissues and 32 precancerous tissues in the TCGA STAD dataset. ZFP1 expression was higher in GC samples ( $p < 0.001$ ) (Fig. 1B), including 27 pairs of data whose pairwise information was tumour-normal ( $p < 0.05$ ) (Fig. 1C). The ROC curve (AUC = 0.816) indicated the potential diagnostic value of ZFP1 in GC (Fig. 1D). We initially examined the expression of ZFP1 protein in clinical samples of GC, and western blot results showed higher ZFP1 expression in tumour tissues than in normal tissues adjacent to the cancer (Fig. 1E). The IHC results showed that ZFP1 was highly expressed in GC tissues (Fig. 1F, G), and the same conclusion was obtained by the HPA database validation (Fig. 1H, I).

### Identification of DEGs in GC

DEGs between high- and low-expression samples of ZFP1 were analysed. We identified 129 distinct DEGs: 101 upregulated and 28 downregulated genes. ( $|\text{LogFC}| > 2$ ,  $p_{\text{adj}} < 0.05$ ). The ggplot2 package (version 3.3.6) was used to visualise the differences in the analysis results and obvious differential genes (Supplementary Fig. S1A–E).

### Association of ZFP1 expression with clinicopathologic characteristics and survival rate

Single-gene logistic regression analysis revealed that ZFP1 expression was associated with poor prognosis (Table 2). Increased ZFP1 expression in GC was positively associated with T stage (T3 and T4 vs. T1 and T2, OR = 2.188), pathologic stage (Stage III & S stage IV vs. Stage I & S stage II, OR = 1.705), and histological grade

Characteristics	Levels	Low expression of ZFP1	High expression of ZFP1	P value
n		187	188	
Age, n (%)	< = 65	81 (21.8%)	83 (22.4%)	0.982
	> 65	102 (27.5%)	105 (28.3%)	
Gender, n (%)	Female	59 (15.7%)	75 (20%)	0.092
	Male	128 (34.1%)	113 (30.1%)	
Anatomic neoplasm subdivision, n (%)	Gastroesophageal junction	24 (6.5%)	17 (4.6%)	0.186
	Cardia/Proximal	28 (7.6%)	20 (5.4%)	
	Fundus/Body	62 (16.9%)	68 (18.5%)	
	Antrum/Distal	64 (17.4%)	74 (20.2%)	
	Stomach (NOS)	3 (0.8%)	3 (0.8%)	
	Other	4 (1.1%)	0 (0%)	
Pathologic T stage, n (%)	T1	16 (4.4%)	3 (0.8%)	<b>0.001</b>
	T2	48 (13.1%)	32 (8.7%)	
	T3	82 (22.3%)	86 (23.4%)	
	T4	40 (10.9%)	60 (16.3%)	
Pathologic N stage, n (%)	N0	62 (17.4%)	49 (13.7%)	0.291
	N1	48 (13.4%)	49 (13.7%)	
	N2	40 (11.2%)	35 (9.8%)	
	N3	31 (8.7%)	43 (12%)	
Pathologic M stage, n (%)	M0	168 (47.3%)	162 (45.6%)	0.505
	M1	11 (3.1%)	14 (3.9%)	
Pathologic stage, n (%)	Stage I	33 (9.4%)	20 (5.7%)	0.064
	Stage II	62 (17.6%)	49 (13.9%)	
	Stage III	69 (19.6%)	81 (23%)	
	Stage IV	15 (4.3%)	23 (6.5%)	
Histologic grade, n (%)	G1	6 (1.6%)	4 (1.1%)	<b>&lt; 0.001</b>
	G2	86 (23.5%)	51 (13.9%)	
	G3	92 (25.1%)	127 (34.7%)	
Histological type, n (%)	Diffuse Type	29 (7.8%)	34 (9.1%)	0.579
	Mucinous Type	9 (2.4%)	10 (2.7%)	
	Not Otherwise Specified	98 (26.2%)	109 (29.1%)	
	Papillary Type	3 (0.8%)	2 (0.5%)	
	Signet Ring Type	7 (1.9%)	4 (1.1%)	
	Tubular Type	40 (10.7%)	29 (7.8%)	
Residual tumor, n (%)	R0	154 (46.8%)	144 (43.8%)	0.664
	R1	9 (2.7%)	6 (1.8%)	
	R2	7 (2.1%)	9 (2.7%)	
Primary therapy outcome, n (%)	PD	39 (12.3%)	26 (8.2%)	0.392
	SD	9 (2.8%)	8 (2.5%)	
	PR	1 (0.3%)	3 (0.9%)	
	CR	117 (36.9%)	114 (36%)	
Reflux history, n (%)	No	96 (44.9%)	79 (36.9%)	0.487
Yes	Yes	19 (8.9%)	20 (9.3%)	
Barretts esophagus, n (%)	No	111 (53.4%)	82 (39.4%)	0.231
Yes	Yes	11 (5.3%)	4 (1.9%)	
H pylori infection, n (%)	No	82 (50.3%)	63 (38.7%)	0.598
Yes	Yes	9 (5.5%)	9 (5.5%)	

**Table 1.** Clinical baseline information of GC patients.

(G3 vs. G1&G2, OR = 2.309) ( $p < 0.05$ ). Overexpression of ZFP1 was significantly correlated with tumour T stage (T4 vs. T1,  $p = 0.003$ ) and histological grade (grade 3 vs. grades 2 and 2,  $P < 0.001$ ) (Supplementary Fig. S2A–E).

ZFP1 (HR = 1.575, 95%CI = 1.129–2.199,  $p = 0.008$ ), age, T stage ( $p = 0.011$ ), N stage ( $p = 0.003$ ), M stage ( $p = 0.004$ ), and pathologic stage ( $p = 0.001$ ) were associated with OS in a univariate Cox regression model. Similar results were obtained using multivariate regression analysis (Table 3).



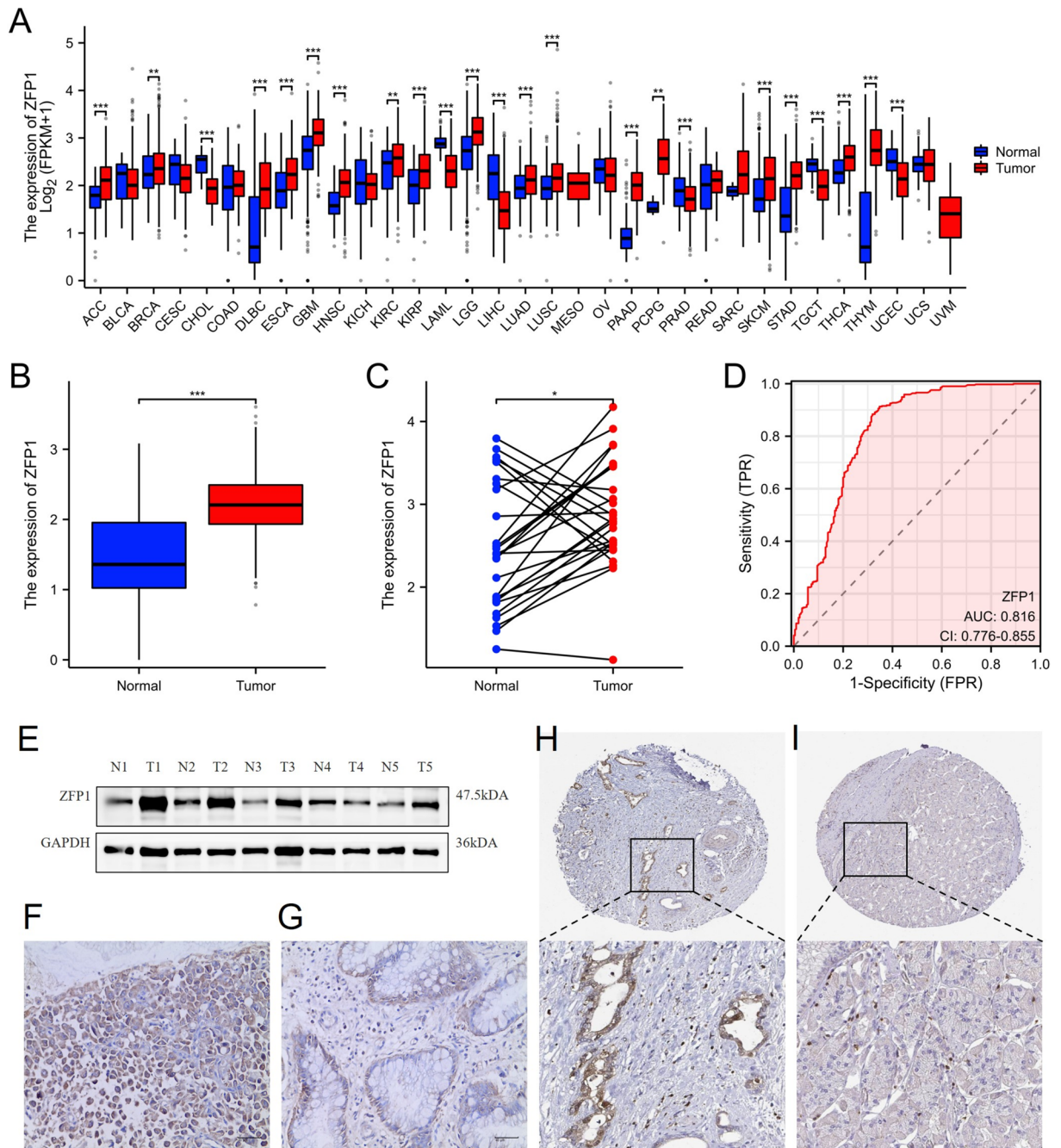


**Fig. 1.** Differential expression of ZFP1 and identification of DEG. (A) Differential expression levels of ZFP1 in different tumor. (B) Expression levels of ZFP1 in GC tissues is higher than normal tissues ( $p < 0.001$ ). (C) Expression levels of ZFP1 in GC tissues is higher than paired adjacent normal tissues ( $p < 0.05$ ). (D) A ROC curve to test the value of ZFP1 to identify GC tissues. ZFP1 protein expression in paired tissues by western blot (E) (full-length blots are presented in Supplementary Fig. 5) and IHC (F, G). Validation of ZFP1 expression in gastric cancer (H) and normal tissues (I) by HPA database.

### The poor prognosis of patients with GC with high ZFP1 expression

Patients with high ZFP1 expression showed significantly lower 10-year OS rates than those with low ZFP1 expression (HR = 1.58,  $p = 0.008$ ; Fig. 2A). Similarly, 10-year DSS (HR = 1.53,  $p = 0.045$ ; Fig. 2B) and PFI (HR = 1.49,  $p = 0.039$ ; Fig. 2C) were significantly lower in patients with high ZFP1 expressing than in those with low ZFP1 expressing. According to subgroup survival analyses of OS, DSS, and PFI, patients with high ZFP1 were more likely to die than those with low ZFP1 (Fig. 2D–L). We conducted a survival analysis of patients with GC based on ZFP1 expression in the GEO database, and the results were consistent (Supplementary Fig. S3A–E).

Characteristics	Total (N)	OR (95% CI)	P value
Pathologic T stage (T3&T4 vs. T1&T2)	367	2.188 (1.711–2.665)	<b>0.001</b>
Pathologic N stage (N1&N2&N3 vs. N0)	357	1.350 (0.900–1.801)	0.191
Pathologic M stage (M1 vs. M0)	355	1.320 (0.501–2.139)	0.506
Pathologic stage (Stage III&Stage IV vs. Stage I&Stage II)	352	1.705 (1.282–2.127)	<b>0.013</b>
Histologic grade (G3 vs. G1&G2)	366	2.309 (1.881–2.738)	< <b>0.001</b>
Primary therapy outcome (PD&SD vs. CR&PR)	317	0.714 (0.206–1.223)	0.195
Residual tumor (R1&R2 vs. R0)	329	1.003 (0.262–1.743)	0.995
Age (> 65 vs. < = 65)	371	1.005 (0.595–1.414)	0.982
Gender (Male vs. Female)	375	0.694 (0.270–1.119)	0.092

**Table 2.** Single-gene logistics regression analysis. Statistically significant values are in [bold].

Characteristics	Total (N)	Univariate analysis		Multivariate analysis	
		Hazard ratio (95% CI)	P value	Hazard ratio (95% CI)	P value
Pathologic T stage	362				
T1 & T2	96	Reference		Reference	
T3 & T4	266	1.719 (1.131–2.612)	<b>0.011</b>	1.099 (0.644–1.875)	0.730
Pathologic N stage	352				
N0 & N1	204	Reference		Reference	
N2 & N3	148	1.650 (1.182–2.302)	<b>0.003</b>	1.262 (0.787–2.024)	0.334
Pathologic M stage	352				
M0	327	Reference		Reference	
M1	25	2.254 (1.295–3.924)	<b>0.004</b>	2.074 (1.057–4.067)	<b>0.034</b>
Pathologic stage	347				
Stage I & Stage II	160	Reference		Reference	
Stage III & Stage IV	187	1.947 (1.358–2.793)	< <b>0.001</b>	1.384 (0.783–2.444)	0.263
Histologic grade	361				
G1 & G2	144	Reference		Reference	
G3	217	1.353 (0.957–1.914)	0.087	1.313 (0.887–1.942)	0.174
Age	367				
< = 65	163	Reference		Reference	
> 65	204	1.620 (1.154–2.276)	<b>0.005</b>	1.909 (1.306–2.792)	< <b>0.001</b>
ZFP1	370				
Low	185	Reference		Reference	
High	185	1.575 (1.129–2.199)	<b>0.008</b>	1.432 (0.994–2.063)	0.054

**Table 3.** Univariate regression analysis of OS using Cox regression model. Statistically significant values are in [bold].

### Nomogram construction and evaluation

Independent prognostic factors for GC were ZFP1 expression level, M stage, and age, based on which a nomogram to predict one-year and three-year survival was constructed (Fig. 3A). Prognostic calibration showed good consistency between the predicted and actual values (Fig. 3B).

### ZFP1 expression and immune infiltration

The high ZFP1 expression group had higher stromal, immune, and estimated scores than the low ZFP1 expression group. (Fig. 4A). The expression of ZFP1 was negatively correlated with IL-17-producing T helper cells (Th17), NK CD56bright cells, and neutrophils and positively correlated with, for example, central memory T cells (Tcm), T helper cells, and Tgd (Fig. 4B–F, Supplementary Fig. S4).

### Protein–protein interaction analysis

To analyse the interactions between upregulated and downregulated DEGs, we constructed a PPI network. As shown in Fig. 5A, the protein regulatory network was divided into five clusters by using the k-means technique. MYC and TRIM28 genes were closely related to ZFP1 in this network.

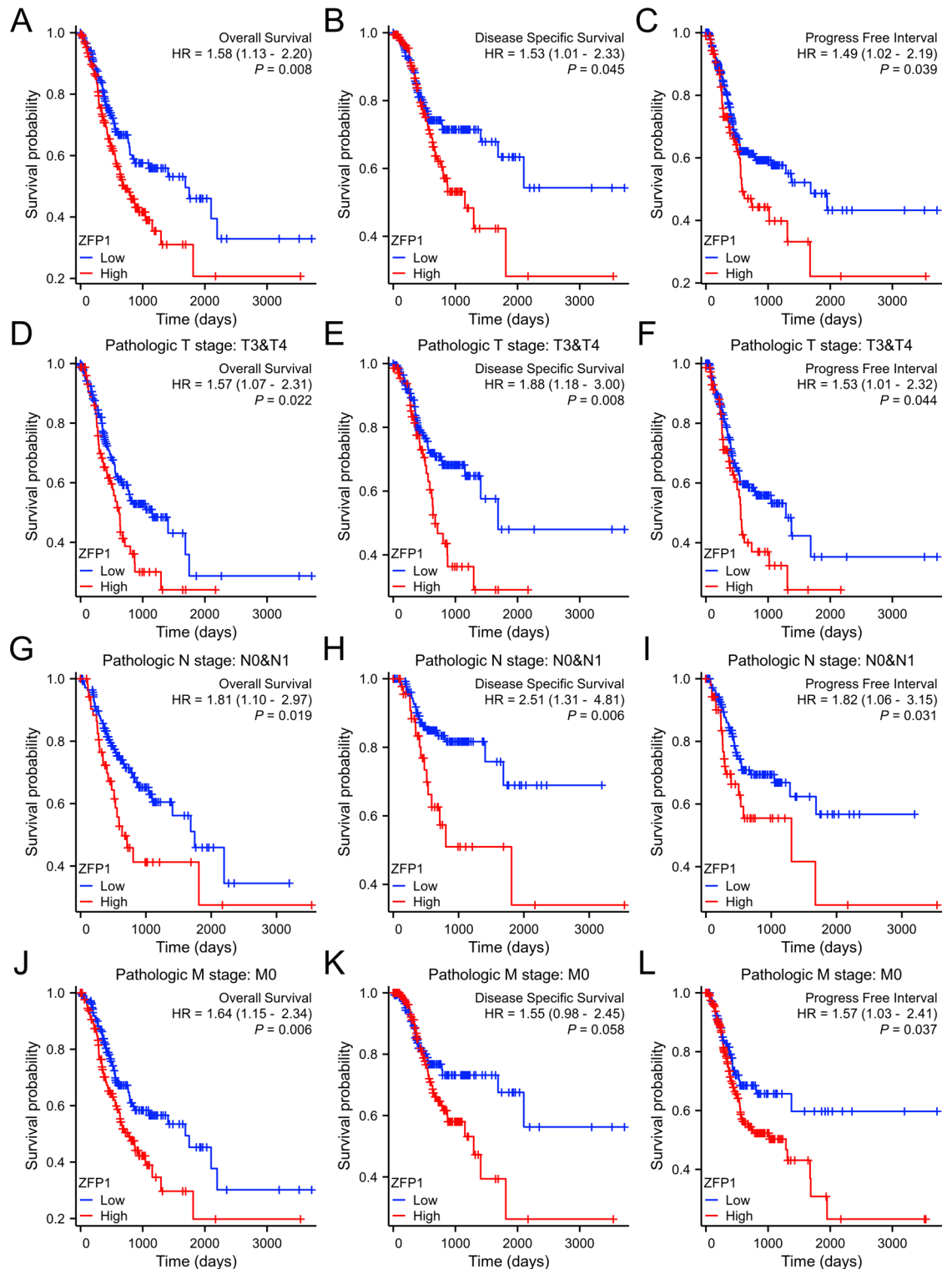


**Fig. 2.** Kaplan–Meier survival curves comparing the high and low expression of ZFP1 in GC. (A–C) Survival curves of OS, DSS, and PFI between ZFP1-high and -low patients with GC. (D–L) Subgroup survival analyses of T3&T4, N0&N1 and M0 were per-formed for OS, DSS and PFI.GC, gastric cancer; OS, overall survival; DSS, disease specific survival; PFI progression free interval.

### Functional enrichment analyses of ZFP1

To forecast ZFP1 interacting genes' functional enrichment information, we performed GO and KEGG enrichment analyses. GO enrichment analysis showed that ZFP1-related genes were involved in biological processes

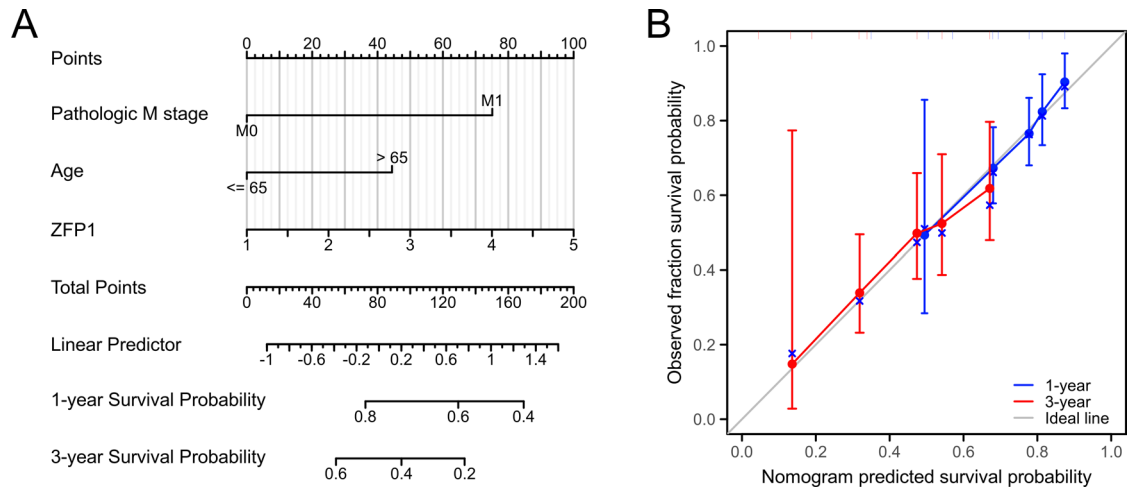


**Fig. 3.** A quantitative method to predict GC patients' probability of 1- and 3-year OS. **(A)** A nomogram for predicting the probability of 1- and 3-year OS for GC patients. **(B)** Calibration plots of the nomogram for predicting the probability of OS at 1- and 3-years. GC, gastric cancer; OS, overall survival.

(BPs), including epidermal cell differentiation, intermediate filament organisation, cell junction assembly, mesenchyme development, and mitochondrial autophagy. Cell composition (CC) mainly includes the collagen-containing extracellular matrix, transporter complex, intermediate filament, cell body membrane, and cell–cell junction. The molecular functions (MFs) mainly included signalling receptor activator activity, interleukin-1 receptor binding, DNA-binding transcription repressor activity, growth factor activity, structural constituents of the cytoskeleton, and cytokine activity (Fig. 5B). KEGG results revealed that DEGs were primarily enriched in fat digestion and absorption, calcium signalling, cGMP-PKG signalling, cAMP signalling, circadian entrainment, AMPK signalling, IL-17 signalling, and MAPK signalling pathways (Fig. 5C).

### GSEA enrichment analysis

The key signalling pathways involved in GC based on differential ZFP1 expression were identified using GSEA ( $p_{\text{adj}} < 0.05$ ,  $\text{FDR} < 0.25$ ) and illustrated meaningful distinctions in the enrichment of MSigDB Collections (c2.cp.all.v2022.1.Hs.symbols.gmt [All Canonical Pathways]). The differentially enriched pathways in the ZFP1 high expression phenotype included ECM receptor interaction, focal adhesion, the PI3K AKT signalling pathway, the MAPK signalling pathway, the Hippo signalling pathway, the integration of energy metabolism, the WNT signalling pathway, and regulation of autophagy (Fig. 6A–I).

### Predicting the lncRNA-miRNA regulatory network of ZFP1

Among the 17 intersecting miRNAs shown in the Wayne diagram, hsa-miR-27a-3p showed the strongest negative correlation with ZFP1 mRNA expression (Fig. 7A, Supplementary Fig. S5A–C). These results indicated that hsa-miR-27a-3p might play a role in regulating ZFP1 expression. Next, the ENCORI database was used to forecast hsa-miR-27a-3p's upstream lncRNAs, and 36 possible lncRNAs were identified (Supplementary Table S1). TCGA GC data were screened to identify highly expressed lncRNAs with poor prognostic value (Supplementary Fig. S5F). According to the competitive endogenous RNA (ceRNA) assumption, lncRNA expression can be increased by competitive binding to miRNAs. We detected lncRNAs positively associated with ZFP1 and negatively associated with hsa-miR-27a-3p (Supplementary Fig. S5D, E). We combined the expression, correlation, and survival analyses, and KCNQ1OT1 may be the most promising lncRNA upstream of the hsa-miR-27a-3p/ZFP1 axis in GC (Fig. 7B). MiRNA pull-down assays showed that intracellular hsa-miR-27a-3p could be conjugated to KCNQ1OT1 and ZFP1 mRNA (Supplementary Fig. S6).

### ZFP1 knockdown affected the proliferation and migration of cancer cells

The low knockdown efficiencies of si-ZFP1-2 and si-ZFP1-3 were screened using WB (Fig. 8A). The CCK8 results showed that ZFP1 knockdown inhibited cell proliferation in a time-dependent manner (Fig. 8B). EdU experiments also confirmed the promoting effect of ZFP1 on GC cell proliferation (Fig. 8C). Similarly, ZFP1 knockdown reduced the colony number (Fig. 9A). ZFP1 inhibition decreased the cell migration (Fig. 9B, C) and invasive capacity (Fig. 9D).

### Discussion

ZFP1 is located at 16:75,119,002–75,172,234 and contains 11 exons. The encoded protein is located in the cytoplasm, nucleus (non-nucleolus), and other regions and belongs to the Krueppel C2H2-type ZFP family, containing the KRAB box. In the *Hidradenitis elegans* cryptic rod nematode, ZFP1 regulates the promoter binding of DAF16 and PHA4 to their direct target genes and is required to control the cross-species longevity pathways of insulin/IGF-1-like signalling (IIS) and dietary restriction (DR)<sup>18</sup>. In a zebrafish model, ZFP1, which has a high degree of sequence unity with humans, activates ZfRev-Erb alpha to participate in developmental regulation<sup>19</sup>.



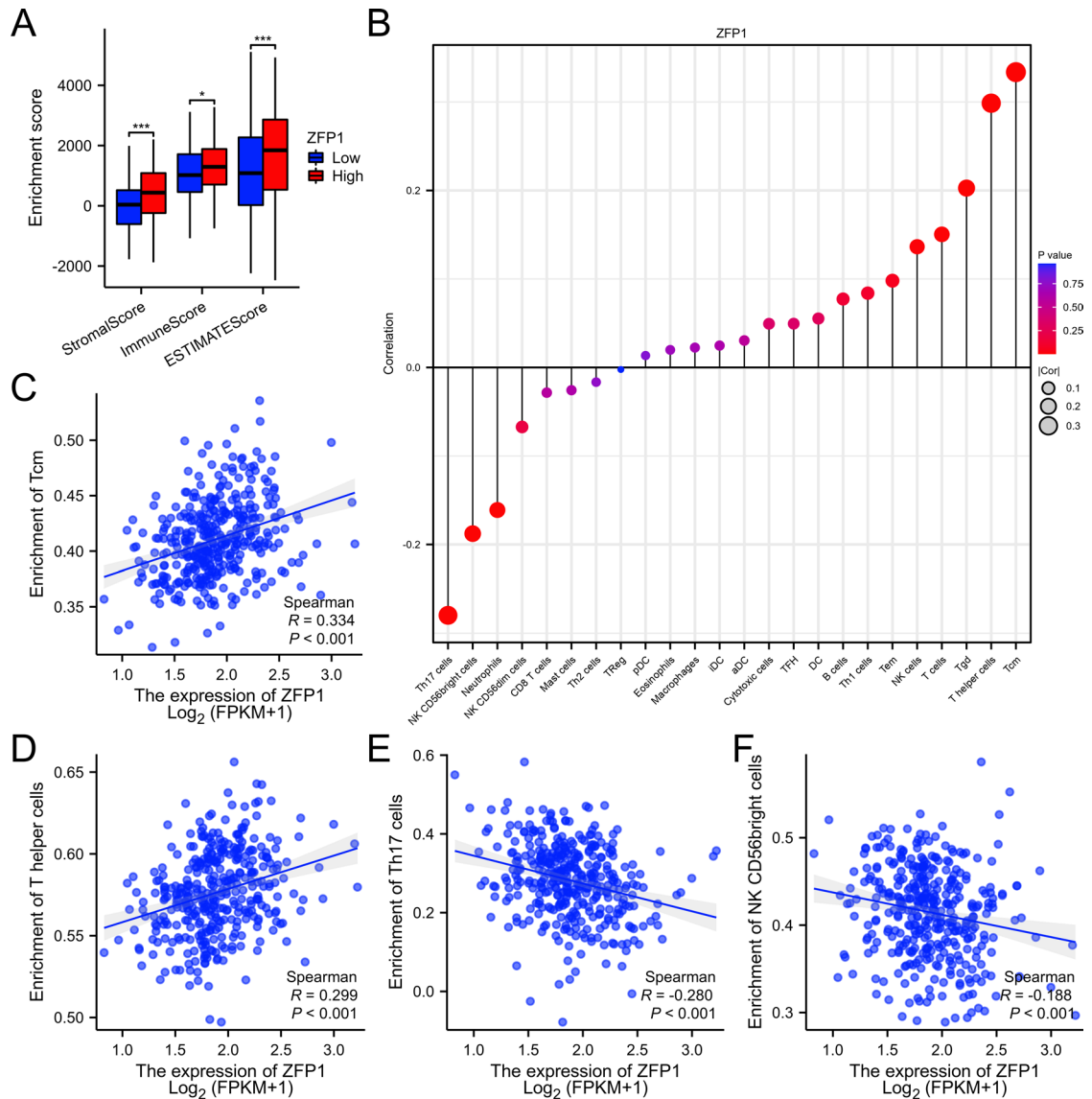


**Fig. 4.** The expression level of ZFP1 is associated with the immune infiltration in GC. **(A)** Gastric cancer tissues with high expression of ZFP1 have higher stromalscore, immunescore and estimatescore. **(B)** Correlation between the relative abundances of 24 immune cells and ZFP1 expression level. **(C–F)** Scatter plots and correlation diagrams showing the difference of Tcm cells helper cells, Th17 cells and NK CD56bright cells infiltration level between ZFP1-high and -low groups.

ZFP1 is involved in regulating mouse embryonic development, and its expression peaks on day 12<sup>7</sup>. Tumours can reactivate regulatory genes during embryonic development as they grow and adapt to environmental stress. The role of ZFP1 as a transcription factor in tumours is understudied, and only the RUSC1-AS1-miR-7-ZFP1 ceRNA axis in laryngeal cancer has been predicted to be involved in tumour progression and is associated with poor prognosis<sup>12</sup>. Regulation of ZFP1 by hsa\_circ\_0008792/hsa-miR-711 in osteosarcoma reduced invasion and promoted apoptosis<sup>20</sup>. However, the relationship between ZFP1 expression and GC has not been reported. Therefore, we investigated the prognostic value and potential mechanisms of ZFP1 in GC in a predictive manner.

We found that ZFP1 expression was increased in many tumours. Clinical samples confirmed that ZFP1 is highly expressed in GC. The AUC value for ZFP1 was 0.816, which is diagnostic for STAD. Univariate logistic regression analysis demonstrated that ZFP1 expression was significantly associated with poor T-staging, late pathological staging, and high histological grade in GC. Survival analysis confirmed that higher ZFP1 expression was associated with shorter patient survival, which was consistent with the validation results from the GEO database. Subgroup analyses revealed that ZFP1 expression was significantly associated with survival at T3, T4, N0, N1, and M0. These results suggest that ZFP1 is probably a new marker for poor prognosis in GC and might be a new target for GC treatment.

Further analyses were performed to investigate the potential role of ZFP1 in STAD progression. GO analysis showed that ZFP1 might be involved in mitochondrial autophagy, an intracellular organelle involved in energy production, cellular metabolism, and cellular signalling. Mitochondrial metabolism is involved in tumour metabolism and the tumour microenvironment<sup>21</sup>. The cAMP signalling pathway involved in the KEGG analysis

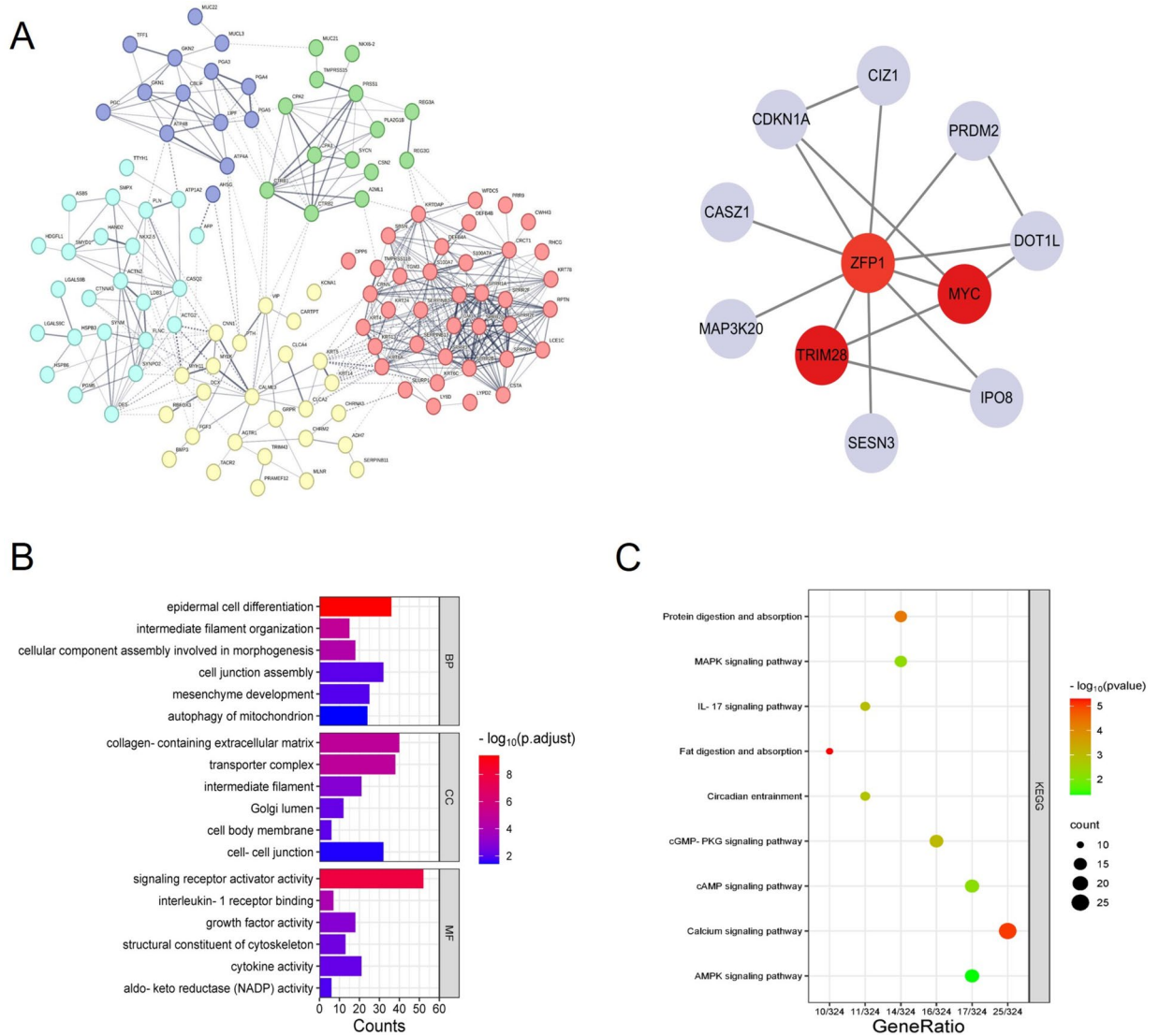


**Fig. 5.** The function network of ZFP1. **(A)** The PPI network associated with ZFP1 in gastric cancer. **(B)** GO enriched terms colored according to P-values. **(C)** Bubble plot showed the KEGG enrichment results of ZFP1.

plays an important role in cellular and systemic energy homeostasis along with the AMPK signalling pathway<sup>22</sup>. Activation of the cAMP signalling pathway promotes mitochondrial metabolism and tumour cell growth<sup>23</sup>.

The results of the GESA suggested that ZFP1 is involved in the regulation of GC progression through multiple mechanisms. The ECM promotes integrin-dependent signalling for invasion and proliferation, induces the formation of favourable microenvironmental ecological niches for metastatic cells, and interferes with cancer-immune cell communication and the formation of physical barriers to anticancer drugs<sup>24</sup>. Hippo kinases (including MST1/2 and LATS1/2) are downregulated, or the downstream genes YAP1 and TAZ are upregulated, promoting the occurrence, progression, and recurrence of GC<sup>25</sup>. The MAPK and PI3K/AKT signalling pathways are abnormally activated in GC<sup>26,27</sup>; play a wide range of regulatory roles in the progression of GC, such as proliferation and metastasis<sup>28</sup>; and are regarded as promising targets for drugs<sup>29</sup>. Notably, both pathways may inhibit autophagy by activating mTOR. There is some controversy regarding the inhibitory or promotional role of autophagy in tumours<sup>30</sup>. Generally accepted is that autophagy plays a deterrent role in the initial stage of tumourigenesis, whereas survival pressure during tumour progression can promote tumour cells to regulate energy allocation through autophagy, facilitating the survival of tumour cells in a hostile environment<sup>31,32</sup>. We predicted that ZFP1 would positively correlate with MAPK, the PI3K/AKT signalling pathway, and autophagy. An in-depth study of the regulatory mechanism of ZFP1 and an elaboration of the interactions between these pathways may provide a reference for explaining this paradoxical relationship.

PPI showed that ZFP1 protein may interact with MYC and TRIM28. MYC is a well-recognised oncogene, and its overexpression in GC tissues regulates key downstream genes and plays multiple roles in promoting tumour progression<sup>33</sup>. In addition, c-MYC can promote GC progression as a major downstream effector of both the MAPK/ERK and PI3K/AKT pathways<sup>34</sup>. TRIM28 can interact with KRAB-ZFP factors to mediate epigenetic regulation and maintain the pluripotency of human embryonic stem cells (hESCs)<sup>35</sup>. In tumour cells, TRIM28



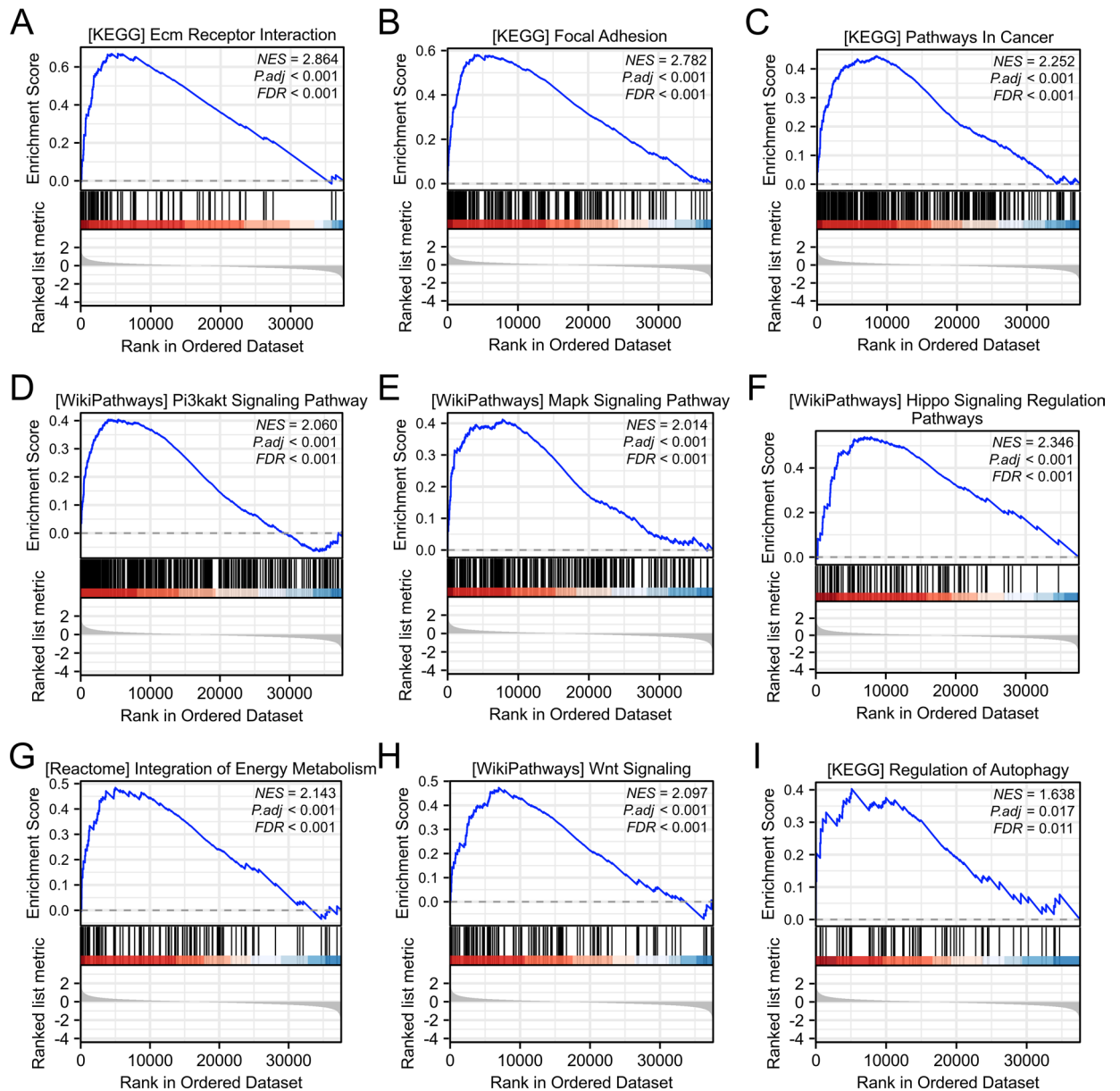


**Fig. 6.** Enrichment plots from Gene Set Enrichment Analysis (GSEA). Several pathways and biological processes were differentially enriched in ZFP1-related GC, including activated ECM receptor interaction, focal adhesion, PI3K AKT signaling pathway, MAPK signaling pathway, Hippo signaling pathway, integration of energy metabolism signaling pathway and regulation of autophagy.

is involved in homeostasis processes such as target gene transcription, downregulation of p53 activity, response to DNA damage, induction of epithelial-to-mesenchymal transition, stemness sustainability, regulation of retrotransposition, and stimulation of autophagy<sup>36</sup>. TRIM28 inhibits PD-L1 ubiquitylation, which results in direct SUMOylation of PD-L1 and increases PD-L1 abundance, allowing GC cells to escape immune surveillance<sup>37</sup>. This suggests a key role for ZFP1 in the regulation of GC and indirectly indicates its involvement in tumour immunity.

Further investigation showed that ZFP1 promotes tumour immune infiltration. In immunoassays, the upregulation of ZFP1 expression was positively correlated with Tcm, T helper cells, and Tgd and negatively correlated

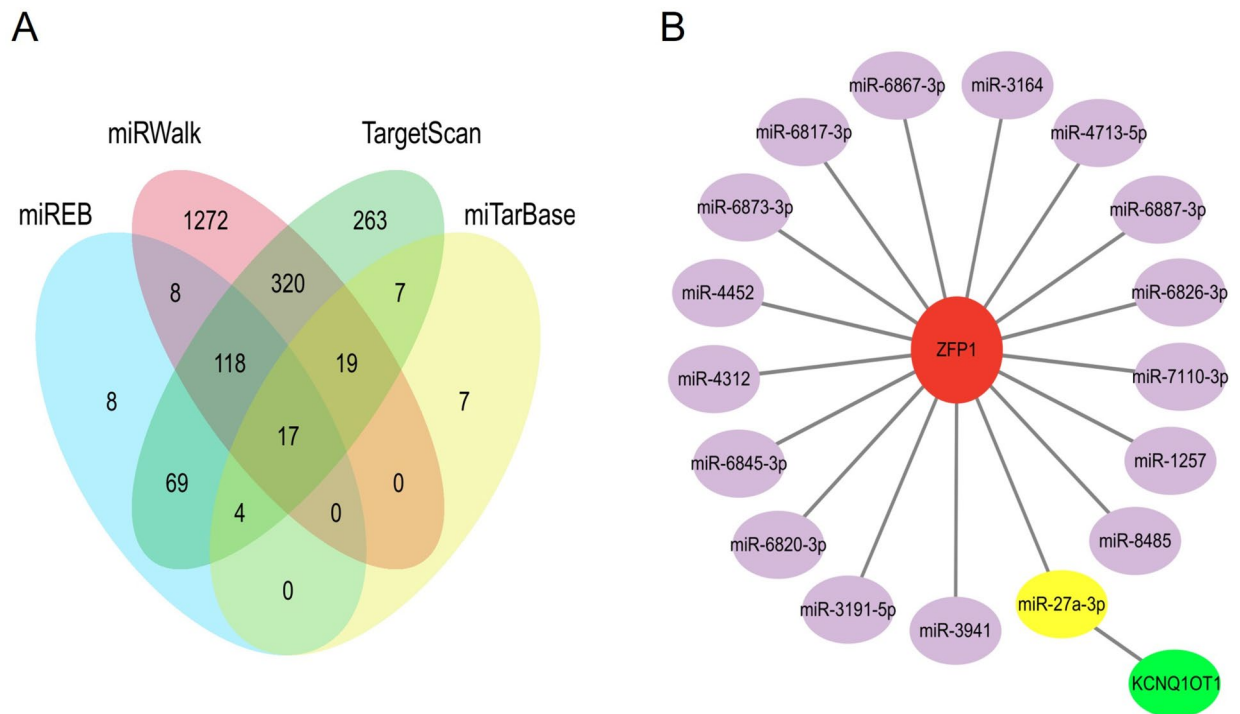


**Fig. 7.** Prediction of lncRNA/miRNA/ZFP1 regulatory network. **(A)** The Venn diagram shows a total of 17 miRNAs that are predicted to regulate ZFP1. **(B)** Prediction and construction of lncRNA/miRNA/ZFP1 regulatory network associated with ZFP1 in GC.

with Th17, NK CD56bright cells, and neutrophils. Once tumours are formed, the tumour-infiltrating effector CD8+ T cells cannot eliminate them, and long-term surviving memory T cells are required to maintain a continuous antitumour immune effect. Memory T cells can be divided into cell populations such as Tcm, Tem, Tscm, and Trm<sup>38</sup>, with Tcm acting as a sentinel in long-term antitumour immunity<sup>39</sup>. After the tumour antigen is recognised, Tcm may be responsible for remembering the tumour antigen and stimulating TEM production. Decreased memory T cells reduce their killing effect on tumours, and tumour cells induce immune escape by inhibiting the expression of memory T cells, increasing their susceptibility to infiltration and metastasis<sup>40</sup>. Th17 cells are a newly discovered subpopulation of Th cells; however, their effects on cancer cells are controversial. An increase in the Treg/Th17 ratio may lead to a decrease in the antitumour immune response<sup>41</sup>. D56bright cells have a potent cytokine-producing capacity and can be potent antitumour effectors when stimulated by pro-inflammatory factors<sup>42</sup>. NK D56dim cells mediate the sequential killing of malignant tumours via granzyme B and perforin<sup>43</sup>. Based on the aforementioned analyses, ZFP1 may play an important role in tumour immunomodulation in STAD. However, the mechanisms and functions of immune cells in the tumour immune microenvironment and tumour progression are complex. Immune cells of the same type are highly heterogeneous and may play diverse roles in different types of pathology, staging, or molecular typing. There may also be synergistic or antagonistic effects between the immune cells. In addition, tumour cells may induce and alter immune cells. However, further studies are required to clarify this.

The lncRNA-miRNA-mRNA axis plays an important role in regulating gastric carcinogenesis and progression<sup>44</sup>. The lncRNA KCNQ1OT1 is involved in the malignant phenotype of multiple tumours and influences GC progression<sup>45</sup>. Although we constructed a model of the KCNQ1OT1/hsa-miR-27a-3p/ZFP1 axis in GC (Fig. 10), further experiments are required to verify the objectivity of this regulatory relationship.

In this study, we predicted the role of ZFP1 in GC based on bioconfidence analysis. We initially proved that ZFP1 is widely involved in the progression of GC, which is expected to be a new target for the diagnosis and treatment of GC. However, the mechanism of ZFP1 involvement in GC progression has not been sufficiently elucidated. Thus, we will continue to study the specific regulatory mechanisms of ZFP1 in GC. Additionally, we need to expand the sample size and further elaborate the relationship between ZFP1 and clinicopathological data.

## Conclusion

In conclusion, ZFP1 may play a critical role in the prognosis, immunity, and progression of GC and be a potential molecule that influences the diagnosis and treatment of GC. Further experiments are required to verify the biological effects of ZFP1 in GC.

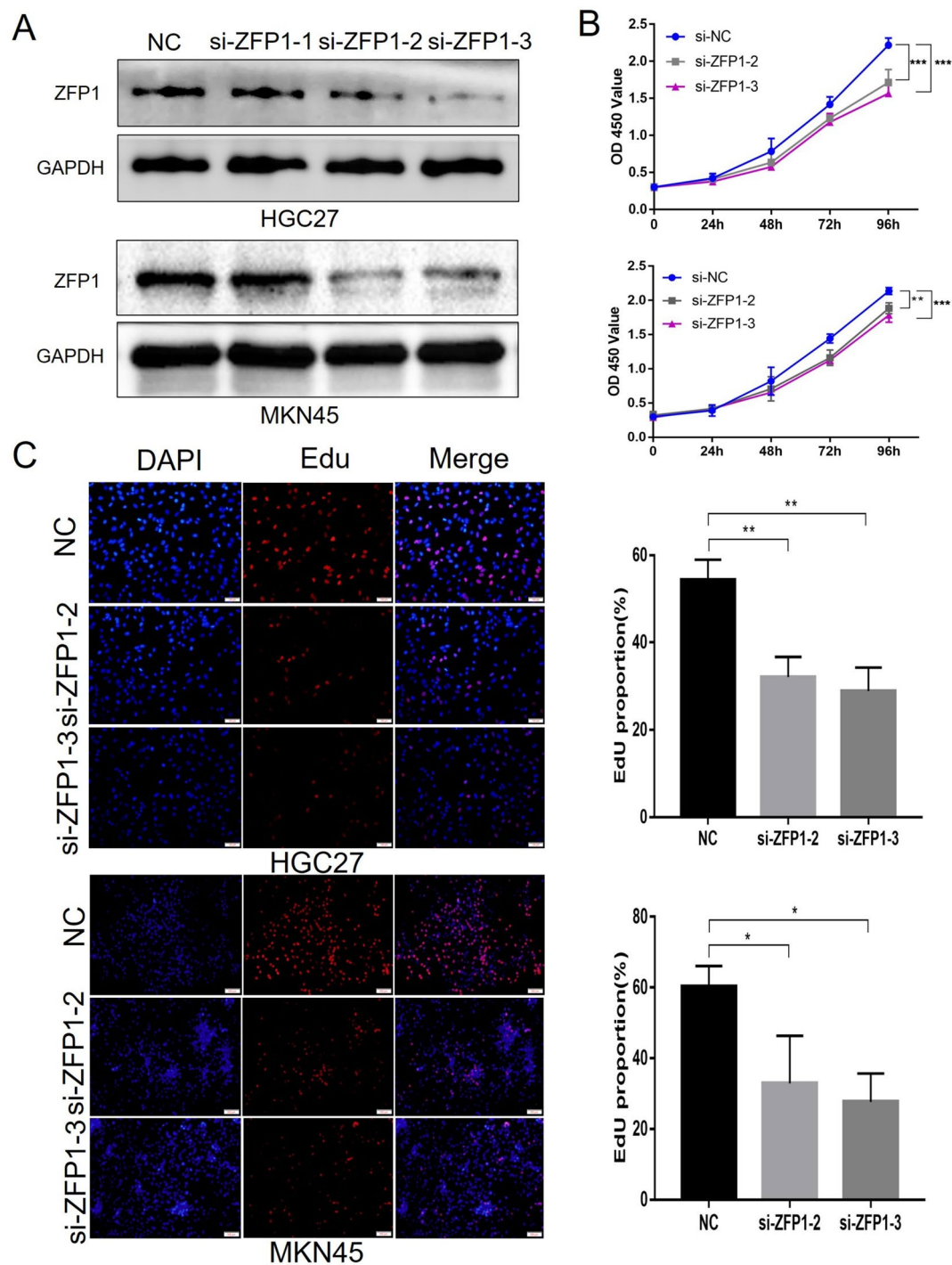


**Fig. 8.** ZFP1 was involved in cell proliferation and migration. (A) ZFP1 knockdown efficiency was assessed by Western blotting on day 3 after transfection with specific ZFP1 siRNAs (full-length blots are presented in Supplementary Fig. 8). (B, C) Cell proliferation ability was evaluated by CCK8 and Edu.

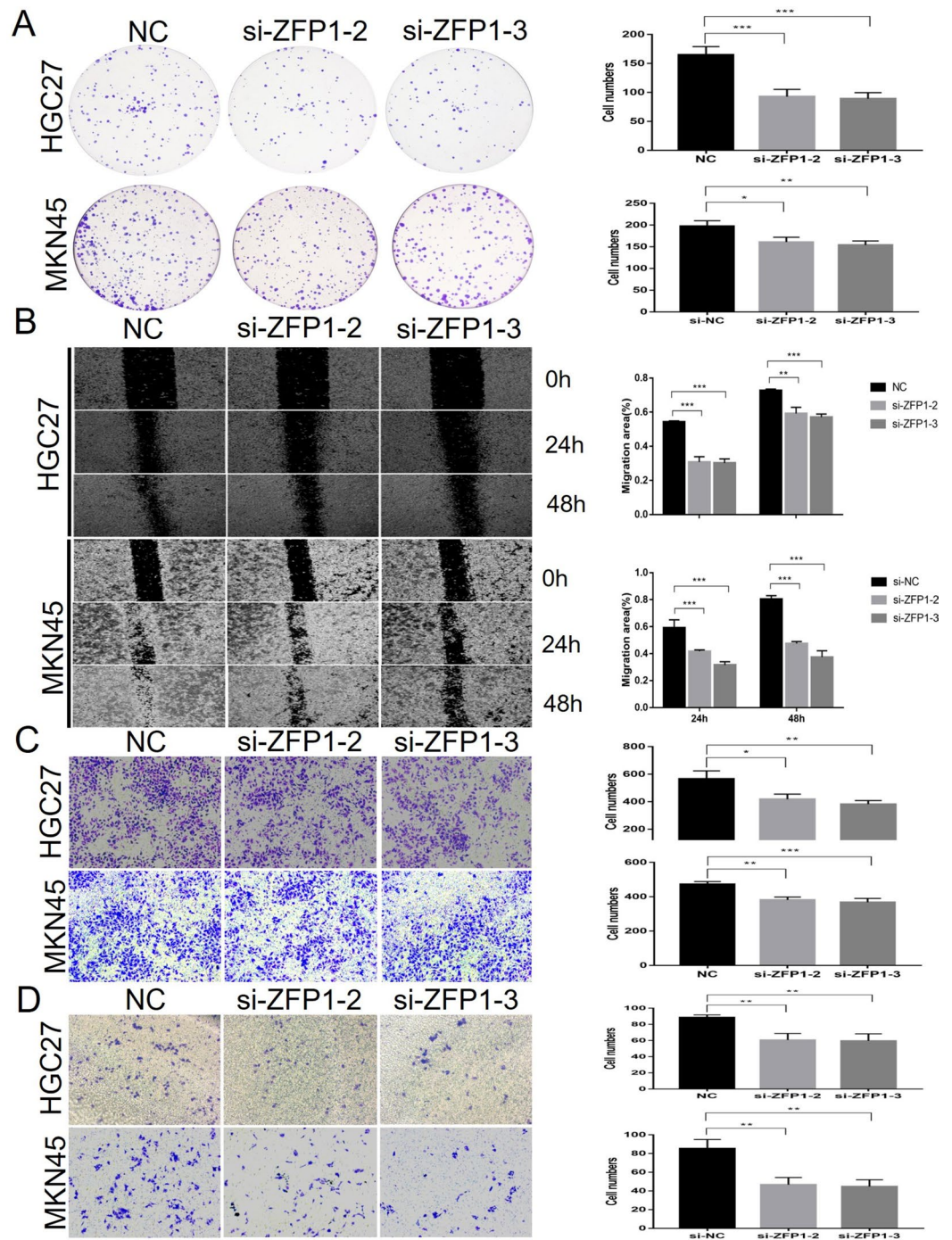


**Fig. 9.** (A) Cell self-renewal and colony formation ability was determined 2 weeks after transfection with ZFP1 siRNAs. (B, C) Scratch and trans well experiments to assess migratory capacity. (D) Invasive capacity assessment.



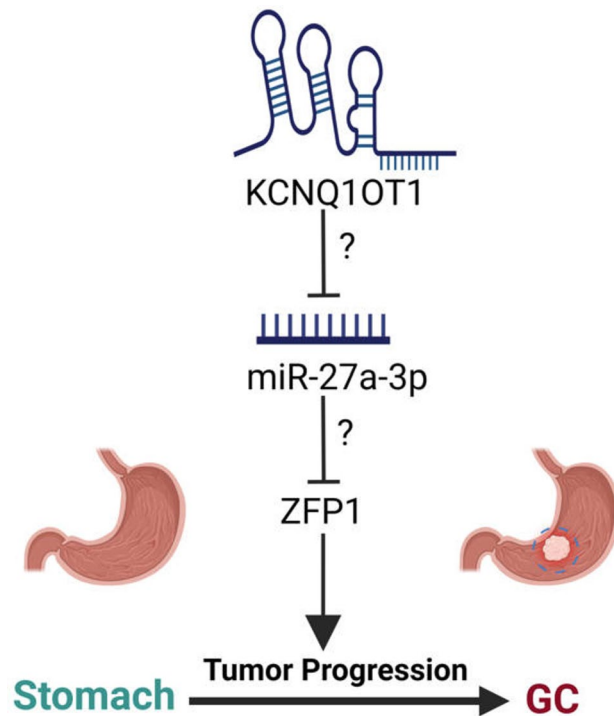


**Fig. 10.** The model of KCNQ1OT1/hsa-miR-27a-3p/ZFP1 axis in carcinogenesis of GC.

### Data availability

The data supporting the results of this study can be obtained from the corresponding author upon reasonable requirements.

Received: 12 April 2024; Accepted: 6 September 2024

Published online: 11 September 2024

### References

- Sung, H. *et al.* Global cancer statistics 2020: GLOBOCAN estimates of incidence and mortality worldwide for 36 cancers in 185 countries. *CA Cancer J. Clin.* **71**, 209–249. <https://doi.org/10.3322/caac.21660> (2021).
- Smyth, E. C., Nilsson, M., Grabsch, H. I., van Grieken, N. C. & Lordick, F. Gastric cancer. *Lancet (Lond., Engl.)* **396**, 635–648. [https://doi.org/10.1016/s0140-6736\(20\)31288-5](https://doi.org/10.1016/s0140-6736(20)31288-5) (2020).
- Joshi, S. S. & Badgwell, B. D. Current treatment and recent progress in gastric cancer. *CA Cancer J. Clin.* **71**, 264–279. <https://doi.org/10.3322/caac.21657> (2021).
- Olechnowicz, A., Oleksiewicz, U. & Machnik, M. KRAB-ZFPs and cancer stem cells identity. *Genes Dis.* **10**, 1820–1832. <https://doi.org/10.1016/j.gendis.2022.03.013> (2023).
- Ecco, G., Imbeault, M. & Trono, D. KRAB zinc finger proteins. *Dev. (Camb. Engl.)* **144**, 2719–2729. <https://doi.org/10.1242/dev.132605> (2017).
- Liu, S., Liu, X., Lin, X. & Chen, H. Zinc finger proteins in the war on gastric cancer: Molecular mechanism and clinical potential. *Cells* **2023**, **12**. <https://doi.org/10.3390/cells12091314> (2023).
- Chowdhury, K., Dietrich, S., Balling, R., Guenet, J. L. & Gruss, P. Structure, expression and chromosomal localization of Zfp-1, a murine zinc finger protein gene. *Nucleic Acids Res.* **17**, 10427–10438. <https://doi.org/10.1093/nar/17.24.10427> (1989).
- Albertsen, M., Teperek, M., Elholm, G., Fuchtbauer, E. M. & Lykke-Hartmann, K. Localization and differential expression of the Kruppel-associated box zinc finger proteins 1 and 54 in early mouse development. *DNA Cell Biol.* **29**, 589–601. <https://doi.org/10.1089/dna.2010.1040> (2010).
- Avgousti, D. C., Cecere, G. & Grishok, A. The conserved PHD1-PHD2 domain of ZFP-1/AF10 is a discrete functional module essential for viability in *Caenorhabditis elegans*. *Mol. Cell Biol.* **33**, 999–1015. <https://doi.org/10.1128/mcb.01462-12> (2013).
- Deutsch, J. L. & Heath, J. L. MLLT10 in benign and malignant hematopoiesis. *Exp. Hematol.* **87**, 1–12. <https://doi.org/10.1016/j.exphem.2020.06.002> (2020).
- Jing, X. *et al.* MLLT10 promotes tumor migration, invasion, and metastasis in human colorectal cancer. *Scand. J. Gastroenterol.* **53**, 964–971. <https://doi.org/10.1080/00365521.2018.1481521> (2018).
- Hui, L., Wang, J., Zhang, J. & Long, J. lncRNA TMEM51-AS1 and RUSC1-AS1 function as ceRNAs for induction of laryngeal squamous cell carcinoma and prediction of prognosis. *PeerJ* **7**, e7456. <https://doi.org/10.7717/peerj.7456> (2019).
- Walter, W., Sánchez-Cabo, F. & Ricote, M. GOrnet: An R package for visually combining expression data with functional analysis. *Bioinform. (Oxf., Engl.)* **31**, 2912–2914. <https://doi.org/10.1093/bioinformatics/btv300> (2015).
- Kanehisa, M., Furumichi, M., Sato, Y., Kawashima, M. & Ishiguro-Watanabe, M. KEGG for taxonomy-based analysis of pathways and genomes. *Nucleic Acids Res.* **51**, D587–d592. <https://doi.org/10.1093/nar/gkac963> (2023).
- Yu, G., Wang, L. G., Han, Y. & He, Q. Y. clusterProfiler: An R package for comparing biological themes among gene clusters. *Omic J. Integr. Biol.* **16**, 284–287. <https://doi.org/10.1089/omi.2011.0118> (2012).
- Yoshihara, K. *et al.* Inferring tumour purity and stromal and immune cell admixture from expression data. *Nat. Commun.* **4**, 2612. <https://doi.org/10.1038/ncomms3612> (2013).

17. Bindea, G. *et al.* Spatiotemporal dynamics of intratumoral immune cells reveal the immune landscape in human cancer. *Immunity* **39**, 782–795. <https://doi.org/10.1016/j.immuni.2013.10.003> (2013).
18. Singh, A. *et al.* A chromatin modifier integrates insulin/IGF-1 signalling and dietary restriction to regulate longevity. *Aging Cell* **15**, 694–705. <https://doi.org/10.1111/ace.12477> (2016).
19. Kakizawa, T. *et al.* Two differentially active alternative promoters control the expression of the zebrafish orphan nuclear receptor gene Rev-erb $\alpha$ . *J. Mol. Endocrinol.* **38**, 555–568. <https://doi.org/10.1677/jme-06-0063> (2007).
20. Chen, L., Shan, Y., Zhang, H., Wang, H. & Chen, Y. Up-regulation of Hsa\_circ\_0008792 inhibits osteosarcoma cell invasion and migration and promotes apoptosis by regulating Hsa-miR-711/ZFP1. *OncoTargets Therapy* **13**, 2173–2181. <https://doi.org/10.2147/OTT.S239256> (2020).
21. Liu, Y. *et al.* An overview: The diversified role of mitochondria in cancer metabolism. *Int. J. Biol. Sci.* **19**, 897–915. <https://doi.org/10.7150/ijbs.81609> (2023).
22. Aslam, M. & Ladilov, Y. Emerging role of cAMP/AMPK signaling. *Cells* **11**, 2022. <https://doi.org/10.3390/cells11020308> (2022).
23. Deng, Z. *et al.* Selective autophagy of AKAP11 activates cAMP/PKA to fuel mitochondrial metabolism and tumor cell growth. *Proc. Natl. Acad. Sci. U. S. A.* **2021**, 118. <https://doi.org/10.1073/pnas.2020215118> (2021).
24. Moreira, A. M. *et al.* The extracellular matrix: An accomplice in gastric cancer development and progression. *Cells* **2020**, 9. <https://doi.org/10.3390/cells9020394> (2020).
25. Liu, X. *et al.* Targeting the hippo pathway in gastric cancer and other malignancies in the digestive system: From bench to bedside. *Biomedicines* **2022**, 10. <https://doi.org/10.3390/biomedicines10102512> (2022).
26. Bagheri, S. K. A. *et al.* The PI3K/Akt/mTOR signaling pathway in gastric cancer; from oncogenic variations to the possibilities for pharmacologic interventions. *Eur. J. Pharmacol.* **898**, 173983. <https://doi.org/10.1016/j.ejphar.2021.173983> (2021).
27. Magnelli, L., Schiavone, N., Staderini, F., Biagioni, A. & Papucci, L. MAP kinases pathways in gastric cancer. *Int. J. Mol. Sci.* **2020**, 21. <https://doi.org/10.3390/ijms21082893> (2020).
28. Fattahi, S., Amjadi-Moheb, F., Tabaripour, R., Ashrafi, G. H. & Akhavan-Niaki, H. PI3K/AKT/mTOR signaling in gastric cancer: Epigenetics and beyond. *Life Sci.* **262**, 118513. <https://doi.org/10.1016/j.lfs.2020.118513> (2020).
29. Morgos, D. T. *et al.* Targeting PI3K/AKT/mTOR and MAPK signaling pathways in gastric cancer. *Int. J. Mol. Sci.* **2024**, 25. <https://doi.org/10.3390/ijms25031848> (2024).
30. Verma, A. K. *et al.* Autophagy paradox of cancer: Role, regulation, and duality. *Oxid. Med. Cell. Longev.* **2021**, 8832541. <https://doi.org/10.1155/2021/8832541> (2021).
31. Yan, R. L. & Chen, R. H. Autophagy and cancer metabolism—the two-way interplay. *IUBMB life* **74**, 281–295. <https://doi.org/10.1002/iub.2569> (2022).
32. Zhang, J. *et al.* Autophagy regulators in cancer. *Int. J. Mol. Sci.* **2023**, 24. <https://doi.org/10.3390/ijms241310944> (2023).
33. Anauate, A. C. *et al.* The complex network between MYC oncogene and microRNAs in gastric cancer: An overview. *Int. J. Mol. Sci.* **2020**, 21. <https://doi.org/10.3390/ijms21051782> (2020).
34. Ren, X. *et al.* SLC39A10 promotes malignant phenotypes of gastric cancer cells by activating the CK2-mediated MAPK/ERK and PI3K/AKT pathways. *Exp. Mol. Med.* **55**, 1757–1769. <https://doi.org/10.1038/s12276-023-01062-5> (2023).
35. Oleksiewicz, U. *et al.* TRIM28 and interacting KRAB-ZNFs control self-renewal of human pluripotent stem cells through epigenetic repression of pro-differentiation genes. *Stem Cell Rep.* **9**, 2065–2080. <https://doi.org/10.1016/j.stemcr.2017.10.031> (2017).
36. Czerwińska, P., Mazurek, S. & Wiznerowicz, M. The complexity of TRIM28 contribution to cancer. *J. Biomed. Sci.* **24**, 63. <https://doi.org/10.1186/s12929-017-0374-4> (2017).
37. Ma, X. *et al.* TRIM28 promotes the escape of gastric cancer cells from immune surveillance by increasing PD-L1 abundance. *Signal Transd. Target. Therapy* **8**, 246. <https://doi.org/10.1038/s41392-023-01450-3> (2023).
38. Galletti, G. *et al.* Two subsets of stem-like CD8(+) memory T cell progenitors with distinct fate commitments in humans. *Nat. Immunol.* **21**, 1552–1562. <https://doi.org/10.1038/s41590-020-0791-5> (2020).
39. Reina-Campos, M. *et al.* Metabolic programs of T cell tissue residency empower tumour immunity. *Nature* **621**, 179–187. <https://doi.org/10.1038/s41586-023-06483-w> (2023).
40. Gebhardt, T., Park, S. L. & Parish, I. A. Stem-like exhausted and memory CD8(+) T cells in cancer. *Nat. Rev. Cancer* **23**, 780–798. <https://doi.org/10.1038/s41568-023-00615-0> (2023).
41. Wang, M. *et al.* Gastric cancer tissue-derived mesenchymal stem cells impact peripheral blood mononuclear cells via disruption of Treg/Th17 balance to promote gastric cancer progression. *Exp. Cell Res.* **361**, 19–29. <https://doi.org/10.1016/j.yexcr.2017.09.036> (2017).
42. Wagner, J. A. *et al.* CD56bright NK cells exhibit potent antitumor responses following IL-15 priming. *J. Clin. Investig.* **127**, 4042–4058. <https://doi.org/10.1172/jci90387> (2017).
43. Myers, J. A. & Miller, J. S. Exploring the NK cell platform for cancer immunotherapy. *Nat. Rev. Clin. Oncol.* **18**, 85–100. <https://doi.org/10.1038/s41571-020-0426-7> (2021).
44. Zeng, X. *et al.* Research progress on the circRNA/lncRNA-miRNA-mRNA axis in gastric cancer. *Pathol. Res. Pract.* **238**, 154030. <https://doi.org/10.1016/j.prp.2022.154030> (2022).
45. Cagle, P., Qi, Q., Niture, S. & Kumar, D. KCNQ1OT1: An oncogenic long noncoding RNA. *Biomolecules* **2021**, 11. <https://doi.org/10.3390/biom11111602> (2021).

## Acknowledgements

All authors would like to appreciate the TCGA and GEO databases for enabling the availability of high-quality data.

## Author contributions

Data analysis: JBY and FBM. Assistants in data analysis: JBY and DHS. Background investigation: JBY, MXD. Data collection: JBY. Experimental execution: JBY, FBM. Project designation, funding, and supervising: JBY and MXD. All authors contributed to the article and approved the submitted version.

## Funding

This study was supported by the Natural Science Foundation of Gansu Province (No. 22JR5RA668) and Gansu Provincial Hospital Intramural Excellent Doctoral Cultivation Programme Project (No. 22GSSYD-4).

## Competing interests

The authors declare no competing interests.

## Additional information

Correspondence and requests for materials should be addressed to M.D.

Reprints and permissions information is available at [www.nature.com/reprints](http://www.nature.com/reprints).



**Publisher's note** Springer Nature remains neutral with regard to jurisdictional claims in published maps and institutional affiliations.

**Open Access** This article is licensed under a Creative Commons Attribution-NonCommercial-NoDerivatives 4.0 International License, which permits any non-commercial use, sharing, distribution and reproduction in any medium or format, as long as you give appropriate credit to the original author(s) and the source, provide a link to the Creative Commons licence, and indicate if you modified the licensed material. You do not have permission under this licence to share adapted material derived from this article or parts of it. The images or other third party material in this article are included in the article's Creative Commons licence, unless indicated otherwise in a credit line to the material. If material is not included in the article's Creative Commons licence and your intended use is not permitted by statutory regulation or exceeds the permitted use, you will need to obtain permission directly from the copyright holder. To view a copy of this licence, visit <http://creativecommons.org/licenses/by-nc-nd/4.0/>.

© The Author(s) 2024